

## Model comparison of Delta and Omega masses in a covariant Faddeev approach

---

### Helios Sanchis-Alepuz\*

*Institut für Physik, Karl-Franzens-Universität Graz, Universitätsplatz 5, 8010 Graz, Austria*  
*E-mail: helios.sanchis-alepuz@uni-graz.at*

### Reinhard Alkofer

*Institut für Physik, Karl-Franzens-Universität Graz, Universitätsplatz 5, 8010 Graz, Austria*  
*E-mail: reinhard.alkofer@uni-graz.at*

### Gernot Eichmann

*Institut für Theoretische Physik, Justus-Liebig-Universität Giessen, D-35392 Giessen, Germany*  
*E-mail: gernot.eichmann@theo.physik.uni-giessen.de*

### Richard Williams

*Departamento de Física Teórica I, Universidad Complutense, 28040 Madrid, Spain*  
*E-mail: richard.williams@fis.ucm.es*

We compute the vector-meson, nucleon and  $\Delta/\Omega$ -baryon masses and their evolution with the current-quark mass using a covariant generalized Bethe-Salpeter equation approach. The interaction kernel is truncated to a dressed gluon exchange. We study the model dependence of our results with the quark-gluon dressing to assess the validity of the truncation.

*International Workshop on QCD Green's Functions, Confinement and Phenomenology*  
*5-9 September 2011*  
*Trento, Italy*

---

\*Speaker.

## 1. Introduction

The covariant approach to bound-state calculations provides a very powerful tool for the study of relativistic two- and three-body bound states. When applied to hadrons, they rely upon the knowledge of QCD Green's functions. The intrinsic sophistication of these equations, however, presents several difficulties in practical applications due to the complexity of taking such calculations beyond the simplest truncation known as Rainbow-Ladder (RL).

It is only in recent years that a unified approach has been reached for the study of mesons and baryons, with quark-diquark calculations [1–5] surpassed by their more intricate three-body description [6–8]. At the same time however, significant technical progress has been made in the covariant treatment of mesons beyond the RL truncation [9–11]. In the case of baryons, these calculations are, due to technical difficulties, so far restricted to particles composed of quarks of the same mass. Therefore it is not feasible for the moment to calculate the plethora of baryon masses, as is done in other approaches such as constituent quark models (see, e.g. [12] and references therein). Nevertheless, one of the main goals of the approach must be to identify the relevance of the different quantum-field-theoretical interaction terms in bound-state phenomena, and in this respect it represents an excellent tool that is complementary to lattice QCD.

So far, the calculation requires to model the quark-gluon interaction via an effective interaction. However, it is interesting to note that studies within RL have been dominated by just one effective interaction, known as the Maris-Tandy model [13, 14]. On the one hand, this dominance is well-earned since this ansatz performs very well indeed. On the other hand, with the swift improvement in our knowledge of QCD Green's functions from both lattice and functional approaches, it is possible to define different effective interactions which, presumably, capture more faithfully some of QCD's features. Note that this is not to say that they will perform better *phenomenologically*. Therefore, before the daunting challenge of bringing covariant baryon studies beyond RL (such as the inclusion of pion-cloud effects and three-body forces) or drawing conclusions about the role of these different contributions, one should thoroughly investigate the model-independent features within a given truncation scheme.

## 2. Framework

### 2.1 Bound-state equations

The covariant description of bound-state equations begins with Dyson's equation for the connected and amputated  $n$ -quark scattering matrix  $T$ :

$$T = K + KG_0T, \quad (2.1)$$

where  $G_0$  is the disconnected  $n$ -quark dressed propagator and  $K$  is the  $n$ -body kernel that details the interaction between the quarks that constitute the bound state.

It is this interaction kernel  $K$  that proves to be challenging. For mesons we must respect chiral symmetry in order to realise the pion as a (pseudo)-Goldstone boson. This gives a precise relationship between the truncation of the quark-propagator Dyson-Schwinger equation (DSE) and the truncation of the 2-body kernel here. The simplest example of a symmetry-preserving kernel is that of Rainbow-Ladder (RL), though more sophisticated kernels have been studied [9–11].

## 2.2 Quark propagator and DSE

The first ingredient for covariant bound-state studies is the dressed quark propagator,

$$S^{-1}(p) = A(p^2) (i\not{p} + M(p^2)) , \quad (2.2)$$

where  $1/A(p^2)$  is the quark wave-function renormalisation and  $M(p^2)$  is the quark mass function. These scalar dressing functions are obtained as solutions to the quark DSE,

$$S^{-1}(p) = Z_2 S_0^{-1} + g^2 Z_{1f} \int \frac{d^4k}{(2\pi)^4} \gamma^\mu S(k) \Gamma^\nu(k, p) D_{\mu\nu}(q) , \quad (2.3)$$

where  $q = k - p$  is the momentum of the exchanged gluon. Here  $S_0^{-1}(p)$  represents the bare inverse quark propagator, obtained from Eq. (2.2) by setting  $A(p^2) = 1$  and  $M(p^2) = m_0$ . This bare mass is related to the renormalised one via  $Z_2 m_0 = Z_2 Z_m m_q$ , with  $Z_2$  and  $Z_m$  the wave-function and quark-mass renormalisation constants, and  $Z_{1f}$  that of the quark-gluon vertex. The cardinal input in the quark propagator DSE (2.3) are the gluon propagator  $D_{\mu\nu}(q)$  and the quark-gluon vertex  $\Gamma^\nu(k, p)$ .

## 2.3 Rainbow-Ladder

The quark-gluon interaction that appears in DSE for the quark reads:

$$Z_{1f} \frac{g^2}{4\pi} D_{\mu\nu}(q) \Gamma_\nu(k, p) . \quad (2.4)$$

In Landau gauge,  $D_{\mu\nu}$  is just the transverse projector  $T_{\mu\nu}(q) = \delta_{\mu\nu} - q_\mu q_\nu / q^2$  multiplied by the scalar gluon dressing function  $Z(q^2)/q^2$ . The quark-gluon vertex  $\Gamma_\nu(k, p)$  is decomposed as twelve Dirac covariants, of which the minimal set in Landau gauge numbers eight. The full vertex can be written as the sum of its bare tree-level part plus a self-energy correction:  $\Gamma_\nu(k, p) = Z_{1f} \gamma_\nu + \Lambda_\nu$ .

The RL truncation requires that we replace the complicated structure of the quark-gluon vertex with the  $\gamma_\mu$  projection of the non-perturbative corrections. Hence Eq. (2.4) becomes

$$Z_{1f} \frac{g^2}{4\pi} T_{\mu\nu}(q) \frac{Z(q^2)}{q^2} (Z_{1f} + \Lambda(q^2)) \gamma_\nu , \quad (2.5)$$

where now  $\Lambda(q^2)$  is the non-perturbative dressing of the  $\gamma_\nu$  part of the quark-gluon vertex, restricted to depend only on the exchanged gluon momentum. The remaining structures are as before. If one wishes to draw a distinction between the gluon dressing  $Z(q^2)$  and the quark-gluon dressings, it can be useful to define the function  $\Gamma_{YM}(q^2) \equiv Z_{1f} + \Lambda(q^2)$ . This distinction is very important because the gluon propagator is by now well-known from both Lattice studies and other functional approaches. However, if one wishes to take a purely phenomenological approach one can instead combine all scalar dressings into one effective running coupling,  $\alpha_{eff}(q^2)$ :

$$Z_{1f} \frac{g^2}{4\pi} D_{\mu\nu}(q) \Gamma_\nu(k, p) = Z_2^2 T_{\mu\nu}(q) \frac{\alpha_{eff}(q^2)}{q^2} \gamma_\nu . \quad (2.6)$$

In all cases, the Dirac structure remains the same, and  $Z_2^2$  follows from the Slavnov-Taylor identities to maintain multiplicative renormalisability. When it comes to discussing the possible impact of effects beyond RL, it is convenient to think in terms of the separate dressing functions  $Z$  and  $\Lambda$ .

The symmetry-preserving two-body kernel corresponding to this yields the ‘ladder’ part of RL. For simplicity we quote this in terms of  $\alpha_{eff}$ ,

$$K^{2\text{-body}} = 4\pi Z_2^2 \frac{\alpha_{eff}(q^2)}{q^2} T_{\mu\nu}(q) \gamma^\mu \otimes \gamma^\nu . \quad (2.7)$$

For the baryon, the three-body kernel  $K^{3\text{-body}}$  is decomposed into a three-quark irreducible contribution  $K_{\text{irr}}^{3\text{-body}}$  and the sum of permuted two-body kernels  $K_{(a)}^{2\text{-body}}$ , with the subscript  $a$  indicating the spectator quark:

$$K^{3\text{-body}} = K_{\text{irr}}^{3\text{-body}} + \sum_{a=1}^3 S_{(a)}^{-1} \otimes K_{(a)}^{2\text{-body}} . \quad (2.8)$$

Note that for mesons the two-body kernel describes quark-antiquark correlations, whilst in the baryon it pertains to quark-quark correlations. Motivated by the success of quark-diquark calculations, we ignore  $K_{\text{irr}}^{3\text{-body}}$ .

## 2.4 Model interaction

When one constructs a model interaction our first constraint is that of perturbation theory. This only fixes the large momentum behaviour, leaving the IR behaviour unspecified. This is typically chosen such that Dynamical Chiral Symmetry Breaking (DCSB) is realised. The chiral condensate, or equivalently the pion decay constant, determines the strength of chiral-symmetry breaking. These are fixed to their phenomenological/experimental values, respectively. With a symmetry preserving truncation protecting the chiral behaviour, such chiral properties are guaranteed and the characteristic  $m_\pi \propto m_q^{1/2}$  behaviour is seen for ‘small’  $m_q$ .

The vector meson mass is similarly determined, to a large degree, by the strength of breaking of chiral symmetry, albeit linearly with respect to the quark mass. That the interaction thus far constructed also works well here is not surprising, since the vector mesons are  $1S$  states and similarly insensitive to  $L.S$  couplings present in the  $\gamma^\mu \otimes \gamma^\mu$  interaction, that in RL are too attractive. Of course, meson bound-states with different quantum numbers are not so easily described. This is particularly true for the ground-state axial vectors which are significantly overbound here.

In the present work we employ two model interactions. In the Maris-Tandy (MT) model [13, 14] the effective running coupling is given by

$$\alpha_{eff}(q^2) = \pi\eta^7 x^2 e^{-\eta^2 x} + \frac{2\pi\gamma_m(1-e^{-y})}{\log[e^2 - 1 + (1+z)^2]}, \quad \begin{aligned} x &= q^2/\Lambda^2, \\ y &= q^2/\Lambda_t^2, \\ z &= q^2/\Lambda_{QCD}^2, \end{aligned} \quad (2.9)$$

and features a Gaussian distribution in the infrared that provides dynamical chiral symmetry breaking. It is characterized by an energy scale  $\Lambda = 0.74$  GeV, fixed to give the pion decay constant, and a dimensionless parameter  $\eta$ . Many ground-state hadron observables have been found to be almost insensitive to the value of  $\eta$  around  $\eta = 1.8$ . The second part reproduces the one-loop running coupling at large, perturbative, momenta. It includes the anomalous dimension  $\gamma_m = 12/(11N_C - 2N_f)$  of the quark propagator, and we use  $\gamma_m = 12/25$ ,  $\Lambda_{QCD} = 0.234$  GeV and  $\Lambda_t = 1$  GeV. Note that we also employ a Pauli-Villars like regulator with a mass scale of 200 GeV. The quark masses at  $\mu = 19$  GeV are 3.7, 85.2, 869 and 3750 MeV for the  $u/d$ ,  $s$ ,  $c$ , and  $b$  quarks, respectively.

The Alkofer-Fischer-Williams (AFW) model [15], on the other hand, is motivated by the desire to account for the  $U_A(1)$ -anomaly by the Kogut-Susskind mechanism. The effective coupling is constructed as the product of the gluon dressing [16] and a model for the non-perturbative behaviour of the quark-gluon vertex [17],

$$\alpha_{eff}(q^2) = \mathcal{C} \left( \frac{x}{1+x} \right)^{2\kappa} \left( \frac{y}{1+y} \right)^{-\kappa-1/2} \left( \frac{\alpha_0 + a_{UV}x}{1+x} \right)^{-\gamma_0} \left( \lambda + \frac{a_{UV}x}{1+x} \right)^{-2\delta_0}. \quad (2.10)$$

The four terms in parentheses are: the IR scaling of the gluon propagator; IR scaling of the quark-gluon vertex; logarithmic running of the gluon propagator; and the logarithmic running of the quark-gluon vertex. Additionally, the last two are constructed to interpolate between the IR and UV behaviour. The remaining terms are defined as follows:

$$\lambda = \frac{\lambda_S}{1+y} + \frac{\lambda_B y}{1+(y-1)^2}, \quad a_{UV} = \pi \gamma_m \left( \frac{1}{\ln z} - \frac{1}{z-1} \right), \quad \begin{aligned} x &= q^2/\Lambda_{YM}^2, \\ y &= q^2/\Lambda_{IR}^2, \\ z &= q^2/\Lambda_{UV}^2, \end{aligned} \quad (2.11)$$

and  $\alpha_0 = 8.915/N_C$ . Here,  $\Lambda_{YM} = 0.71$  GeV is the dynamically generated Yang-Mills scale, while  $\Lambda_{UV} = 0.5$  GeV corresponds to the one-loop perturbative running. The IR scaling exponent is  $\kappa = 0.595353$ , and the one-loop anomalous dimensions are related via  $1 + \gamma_0 = -2\delta_0 = \frac{3}{8} N_C \gamma_m$ , with  $\gamma_m = 12/(11N_C - 2N_f)$ . We choose  $N_f = 5$  active quark flavours at the renormalisation point  $\mu = 19$  GeV. The constant  $\mathcal{C} = 0.968$  is chosen such that  $\alpha_{eff}$  runs appropriately in the UV. Finally,  $\Lambda_{IR} = 0.42$  GeV,  $\lambda_S = 6.25$ , and  $\lambda_B = 21.83$  determine the IR properties of the quark-gluon vertex and are fitted such that the properties of  $\pi$ ,  $K$  and  $\rho$  mesons are well reproduced. The quark masses at  $\mu = 19$  GeV are 2.76, 55.3, 688 and 3410 MeV for the  $u/d$ ,  $s$ ,  $c$ , and  $b$  quarks, respectively.

### 3. Results and discussion

Using the techniques described in [7, 8], we calculated the vector-meson, nucleon, and delta<sup>1</sup> masses up to the bottom region using the AFW and MT effective interactions. The results are collected in Table 1, and their evolution with the pseudoscalar mass (or, equivalently, with the current-quark mass) is shown in Fig. 1.

Studying different interactions allows to quantify the model dependence within the rainbow-ladder truncation. We find that the two interaction models yield similar overall trends in the results. There is little deviation in the resulting hadron masses in the light-quark region, whereas the MT results tend to underestimate the AFW values for heavier quark masses. In all cases, the agreement with experimental and lattice data is  $\lesssim 10\%$  and comparable to the frequently studied model dependence in the MT interaction that is induced by the parameter  $\eta$ .

We note that both AFW and MT interactions, which were designed in a different spirit, show a qualitatively similar behavior in the mid-momentum range around  $|q| \sim 0.5 \dots 1$  GeV which is the relevant domain for dynamical chiral symmetry breaking. It is this region that provides the overall strength to ground-state hadron properties, whereas their features are less sensitive to the deep-infrared region. The same observation has also been made in recent studies exploring the impact of different model interactions in the light-meson sector [21, 22].

<sup>1</sup> Assuming isospin symmetry,  $\Delta$  and  $\Omega$  baryons have the same structure, changing only the current-quark mass.

$J^{PC} = 0^{-+}$	MT	AFW	exp.
$n\bar{n}$ ( $\pi$ )	0.140 $\dagger$	0.139 $\dagger$	0.138
$n\bar{s}$ ( $K$ )	0.496 $\dagger$	0.497 $\dagger$	0.496
$s\bar{s}$	0.697	0.686	–
$c\bar{c}$ ( $\eta_c$ )	2.979 $\dagger$	2.980 $\dagger$	2.980
$b\bar{b}$ ( $\eta_b$ )	9.388 $\dagger$	9.390 $\dagger$	9.391
$J^{PC} = 1^{--}$	MT	AFW	exp.
$n\bar{n}$ ( $\rho$ )	0.743	0.710	0.775
$n\bar{s}$ ( $K^*$ )	0.942	0.961	0.892
$s\bar{s}$ ( $\phi$ )	1.075	1.114	1.020
$c\bar{c}$ ( $J/\psi$ )	3.163	3.302	3.097
$b\bar{b}$ ( $\Upsilon$ )	9.466	9.621	9.460

	MT	AFW	exp.	
$N$	0.94	0.97	0.94	
$\Delta$	1.26	1.22	1.23	
$\Omega$	1.72	1.80	1.67	
	MT	AFW	lattice	LPW
$\Omega_{ccc}$	4.4	4.9	4.7	4.9(0.25)
$\Omega_{bbb}$	13.7	13.8	14.4	14.5(0.25)

Table 1: Computed meson and baryon masses (GeV) for both MT and AFW interactions, compared to experiment. Quantities fitted to their experimental values are indicated by a  $\dagger$ . Since the heavy-Omega baryons have not been observed yet, we compare to lattice calculations [18, 19] and a recent study from pNRQCD [20].

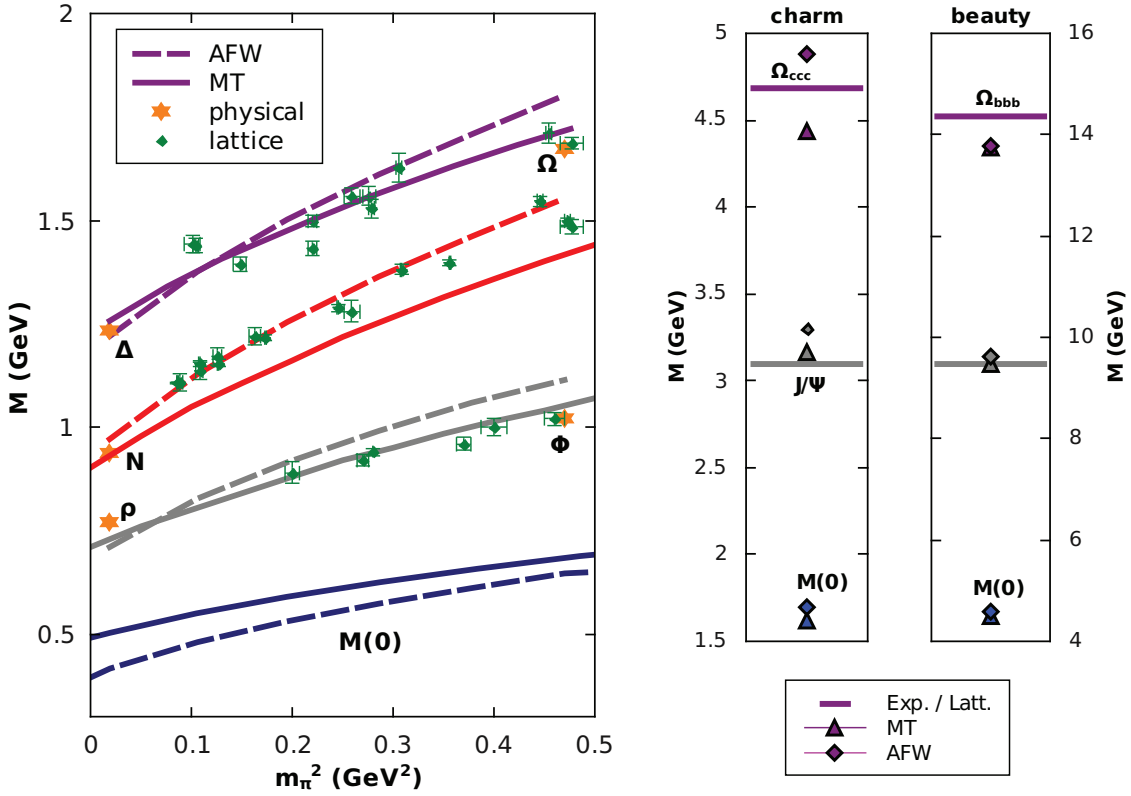


Figure 1: *Left panel:* evolution of  $M(0)$  as well as  $\rho$ ,  $N$  and  $\Delta$  masses with the squared pion mass for MT and AFW models. Results are compared to lattice data; see [7, 8] for references. *Right panel:* vector-meson and triply-heavy omega masses for the two interaction models MT and AFW.

On the other hand, the impact of DCSB is reduced in the heavy-quark domain where hadron properties become increasingly sensitive to the heavy quark mass. We have included the value of the quark mass function  $M(p^2 = 0)$  in both panels of Fig. 1. Since in the heavy-quark limit the variation of  $M(p^2)$  at low momentum is small, its value is indicative of the heavy-quark constituent mass. Indeed we find that the spread between the AFW and MT results in the vector-meson and delta channels in the charm and bottom regions follows the same pattern as that of  $M(0)$ , indicating that their properties are dominated by the features of the quark DSE rather than the details of the effective interaction and the structure of the  $qq$  kernel that enters the bound-state equations.

In that respect it is interesting to speculate about possible effects beyond the RL truncation. Such contributions refer to corrections in the quark-gluon vertex as well as additional structures beyond the vector-vector interaction. Amongst others, they may consist of attractive pion-cloud corrections in the chiral regime, or repulsive corrections from self-interactions of the gluon. They have a two-fold effect: firstly, they allow for non vector-vector interactions and a more general momentum dependence; and secondly, they introduce a quark-mass dependence in the interaction due to the internal quark propagators that are coupled there. This last point is certainly of relevance when trying to describe such a wide range of mass scales provided by the  $u/d$  to  $b$  quarks.

In rainbow-ladder, vertex corrections beyond  $\gamma_v$  are included in the modelling; otherwise Dynamical Chiral Symmetry Breaking would be absent. Since this is done for the light-meson sector, it implies also that only light quark-dynamics are included. As a result, to determine how much room there is for beyond-RL effects, one must consider removing those vertex corrections that are implicitly included. Likely, this can only be achieved for the heavy-quark sector where one expects vertex corrections to be suppressed. This will be considered in a future work.

#### 4. Summary and conclusions

We have studied the quark-mass dependence of several meson and baryon masses in the RL truncated Dyson-Schwinger approach. We investigated a broad range of current-quark masses from the light-quark domain up to the bottom region. To identify model-independent features, we employed two different effective interactions for the quark-(anti)quark kernel. We find that both models yield comparable results that agree with experimental and lattice data within  $\lesssim 10\%$  throughout the quark-mass range, thereby demarcating the model sensitivity within a RL truncation.

The impact of beyond-RL corrections, on the other hand, is easier to access in form-factor studies where they are needed for a correct description in the chiral and low-momentum region. In that respect it is desirable to perform a model comparison of nucleon and delta electromagnetic form factors in the covariant three-body framework. Work in this direction is in progress.

#### Acknowledgments

We thank Christian Fischer, Felipe Llanes-Estrada and Selym Villalba-Chavez for helpful discussions. This work was supported by the Austrian Science Fund FWF under Projects No. P20592-N16, Erwin-Schrödinger-Stipendium J3039, and the Doctoral Program W1203; Ministerio de Educación No. SB2010-0012; as well as in part by the European Union (HadronPhysics2 project “Study of strongly-interacting matter”).

## References

- [1] G. Hellstern, R. Alkofer, M. Oettel and H. Reinhardt, Nucl. Phys. A **627** (1997) 679 [hep-ph/9705267].
- [2] M. Oettel, G. Hellstern, R. Alkofer and H. Reinhardt, Phys. Rev. C **58** (1998) 2459 [nucl-th/9805054].
- [3] J. C. R. Bloch, C. D. Roberts, S. M. Schmidt, A. Bender and M. R. Frank, Phys. Rev. C **60** (1999) 062201 [nucl-th/9907120].
- [4] D. Nicmorus, G. Eichmann, A. Krassnigg and R. Alkofer, Phys. Rev. D **80** (2009) 054028 [arXiv:0812.1665 [hep-ph]].
- [5] D. Nicmorus, G. Eichmann and R. Alkofer, Phys. Rev. D **82** (2010) 114017 [arXiv:1008.3184 [hep-ph]].
- [6] G. Eichmann, R. Alkofer, A. Krassnigg and D. Nicmorus, Phys. Rev. Lett. **104** (2010) 201601 [arXiv:0912.2246 [hep-ph]].
- [7] G. Eichmann, Phys. Rev. D **84** (2011) 014014 [arXiv:1104.4505 [hep-ph]].
- [8] H. Sanchis-Alepuz, G. Eichmann, S. Villalba-Chavez and R. Alkofer, Phys. Rev. D **84** (2011) 096003 [arXiv:1109.0199 [hep-ph]].
- [9] C. S. Fischer and R. Williams, Phys. Rev. D **78** (2008) 074006 [arXiv:0808.3372 [hep-ph]].
- [10] C. S. Fischer and R. Williams, Phys. Rev. Lett. **103** (2009) 122001 [arXiv:0905.2291 [hep-ph]].
- [11] L. Chang and C. D. Roberts, Phys. Rev. Lett. **103** (2009) 081601 [arXiv:0903.5461 [nucl-th]].
- [12] W. Plessas and T. Melde, AIP Conf. Proc. **1056** (2008) 15 [arXiv:0811.1752 [hep-ph]].
- [13] P. Maris and C. D. Roberts, Phys. Rev. C **56** (1997) 3369 [nucl-th/9708029].
- [14] P. Maris and P. C. Tandy, Phys. Rev. C **60** (1999) 055214 [nucl-th/9905056].
- [15] R. Alkofer, C. S. Fischer and R. Williams, Eur. Phys. J. A **38** (2008) 53 [arXiv:0804.3478 [hep-ph]].
- [16] R. Alkofer, W. Detmold, C. S. Fischer and P. Maris, Phys. Rev. D **70** (2004) 014014 [hep-ph/0309077].
- [17] R. Alkofer, C. S. Fischer, F. J. Llanes-Estrada and K. Schwenzer, Annals Phys. **324** (2009) 106 [arXiv:0804.3042 [hep-ph]].
- [18] T. -W. Chiu and T. -H. Hsieh, Nucl. Phys. A **755** (2005) 471 [hep-lat/0501021].
- [19] R. Lewis, AIP Conf. Proc. **1374** (2011) 581 [arXiv:1010.0889 [hep-lat]].
- [20] F. J. Llanes-Estrada, O. I. Pavlova and R. Williams, [arXiv:1111.7087 [hep-ph]].
- [21] M. Blank, A. Krassnigg and A. Maas, Phys. Rev. D **83** (2011) 034020 [arXiv:1007.3901 [hep-ph]].
- [22] S.-X. Qin, L. Chang, Y.-X. Liu, C. D. Roberts and D. J. Wilson, Phys. Rev. C **84** (2011) 042202 [arXiv:1108.0603 [nucl-th]].